Supplementary Information

Phase separation modulates the assembly and dynamics of a polarity related scaffold-signaling hub

Wei Tan[1,#], Sihua Cheng[1,#], Yingying Li[1,#], Xiao-Yang Li[1,2], Ning Lu[1], Jingxian Sun[1], Guiyue Tang[1], Yujiao Yang[3,4], Kezhu Cai[1,5], Xuefei Li[1], Xijun Ou[6], Xiang Gao[1], Guo-Ping Zhao[1,3,7], W. Seth Childers[8], Wei Zhao[1,*]

Supplementary figures:

Supplementary tables:

Supplementary Table 1. Screening of PodJ client proteins in *E. coli*.

Supplementary Table 2. Screening of the regulators of PodJ subcellular localization in *E. coli*.

Supplementary Table 3. Bacterial strains used in this study.

Supplementary Table 4. Plasmids used in this study.

Supplementary Table 5. Oligonucleotides used in this study.

Supplementary Table 6. Constructions of His-tagged proteins used in this study.

Supplementary references

Supplementary figures

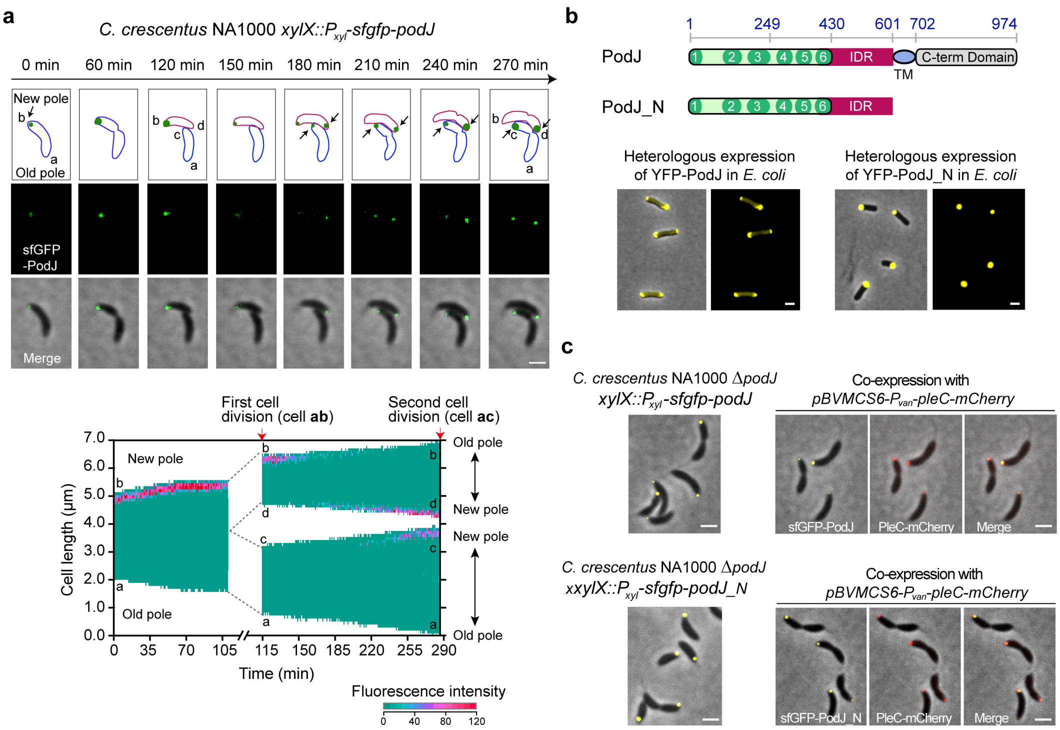

Supplementary Figure 1. **PodJ accumulation in *C. crescentus* and *E. coli*. a**, PodJ specifically accumulates at the new cell poles during the cell cycle. The two cell poles were distinguished by observation of the stalk at the old cell pole. A sole copy of *sfgfp-podJ* in the chromosome was induced by adding 0.003% (w/v) xylose 1 h prior to cell synchronization. Kymographs of the sfGFP-PodJ signal along the cell length over time are shown on the lower panel. Images were acquired every 2 min for *C. crescentus* cells on a PYE pad. The black arrow (upper panel), new cell pole. The red arrow (lower panel), the time point of cell division. **b**, YFP-PodJ_N (YFP-PodJ$_{1\text{-}601}$) accumulates at the cell poles in *E. coli.* Compared with the bipolar localization of YFP-PodJ, YFP-PodJ_N accumulates in a monopolar pattern in *E. coli* for unknown reasons. **c**, sfGFP-PodJ_N accumulates as the full-length YFP-PodJ in *C. crescentus.*

Fluorescence microscopy suggests that sfGFP-PodJ_N accumulates at the new cell pole and recruits a signaling protein (PleC-mCherry) as the full-length sfGFP-PodJ. PodJ and PleC were induced by 0.003% (w/v) xylose and 500 µM vanillate, respectively. All scale bars, 2 µm.

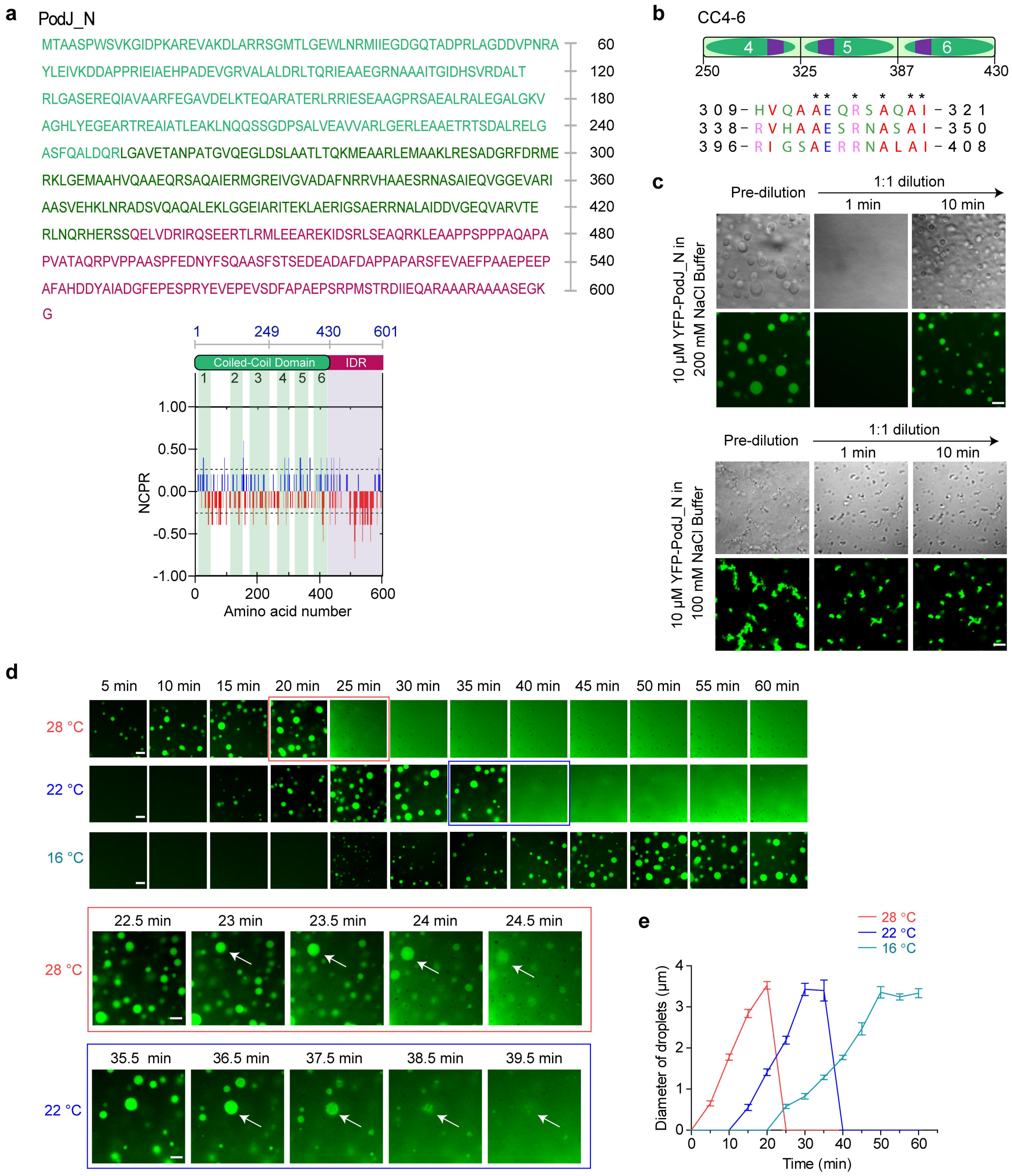

Supplementary Figure 2. Biophysical analyses of YFP-PodJ_N droplets in vitro. **a,** Amino acid sequence analyses of PodJ_N reveal that the IDR domain is rich in negatively charged residues. The PodJ domains of CC1-3, CC4-6, and IDR are colored in light green, dark green, and magenta, respectively (upper panel). CIDER[1] was used for analyzing the net charge per residue (NCPR) distribution of PodJ_N (lower panel). The NCPR plots of positively charged and negatively charged residues are indicated as blue and red, respectively. **b,** Characterization of tandem repeats in $PodJ_{CC4\text{-}6}$. Three tandem repeats (purple) characterized as AE#R#A#AI are identified in the CC4-6 domain of PodJ. *, conserved amino acid in the tandem repeats; #, random amino acid. **c**, Reversible liquid droplets are formed by YFP-PodJ_N in a HEPES buffer (pH 7.5) containing 200 mM NaCl. YFP-PodJ_N droplets dissolved after 1:1 dilution and reassembled in 10 min in a HEPES buffer (pH 7.5) containing 200 mM NaCl. In contrast, YFP-PodJ_N in a HEPES buffer (pH 7.5) containing 100 mM NaCl formed amorphous structures which did not dissolved in the same buffer. **d**, The YFP-PodJ_N droplets emerge and disassemble faster at higher temperatures. The dynamics of YFP-PodJ_N droplets (5 μM) was monitored at different temperatures in a HEPES buffer (pH 7.5) containing 200 mM NaCl. Details of the droplet disassembly are shown with enlarged rectangles, revealing a different pattern from wetting (a phenomenon when biomolecular condensates flatten against a surface[2,3]). Arrow, the disassembling droplets. **e**, Diameter quantification of YFP-PodJ_N droplets in panel d. YFP-PodJ_N droplets (*n* = 677, 551, and 1,802 droplets, respectively; from high to low temperatures) from three independent experiments were measured. Data are means ± SEM. All scale bars, 4 μm. Source data are provided in the Source Data file.

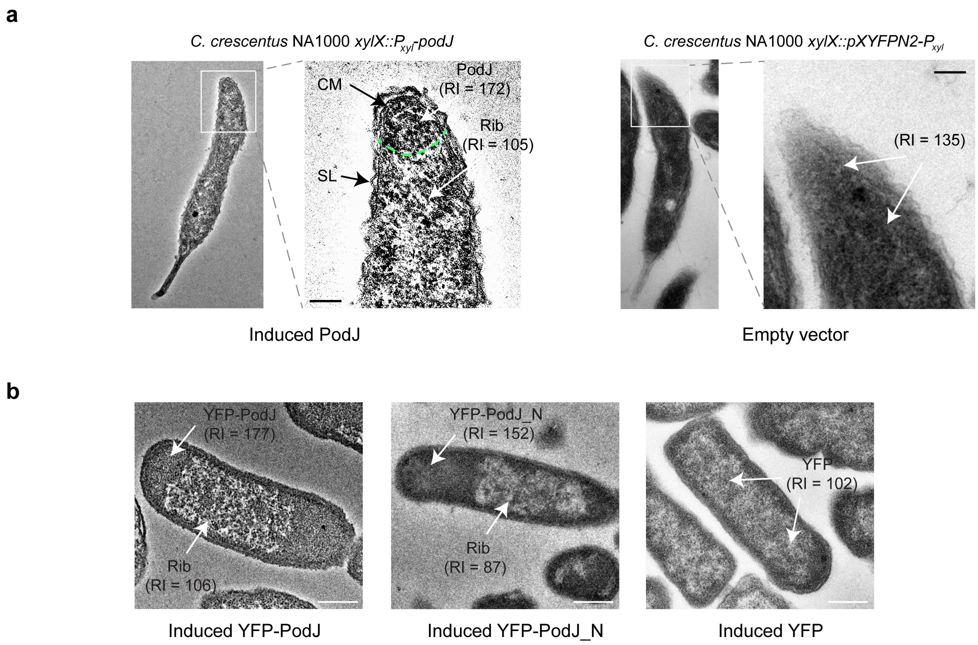

Supplementary Figure 3. Cell compartments are formed in living cells expressing PodJ or PodJ_N. a, TEM analysis of *C. crescentus* cells expressing PodJ (left panel) or empty vector (right panel). Both cells were induced with 0.03% (w/v) xylose for 4 hours before they were fixed. The electron density was measured as relative intensity (RI) using ImageJ. SL, surface layer; CM, cell membrane; PodJ, PodJ accumulation at the pole; Rib, ribosomes and other cell components. Scale bars, 100 nm. **b,** TEM analyses suggest that the PodJ proteins packed into the *E. coli* cell poles. *E. coli* cells expressing YFP-PodJ (left), YFP-PodJ_N (middle), and YFP (right), were induced with 0.1 mM IPTG at 37 °C for 2 h before fixation. All scale bars, 500 nm.

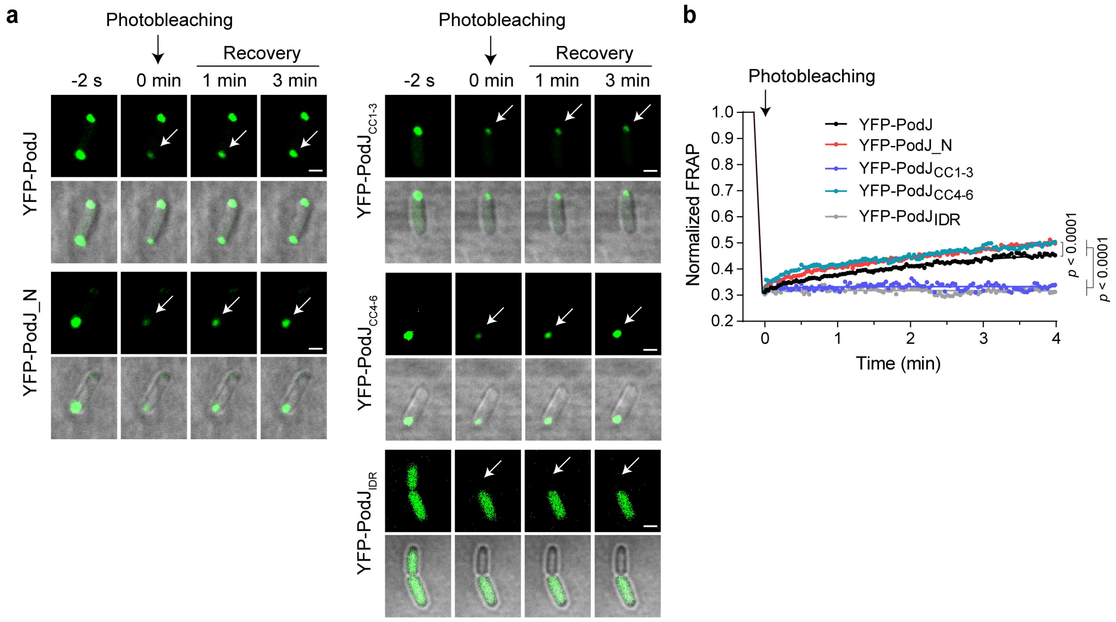

Supplementary Figure 4. CC4-6 is responsible for the formation of PodJ condensates in *E. coli*. a, FRAP analyses demonstrate that the fluorescence intensities of YFP-PodJ, YFP-PodJ_N, and YFP-PodJ$_{CC4-6}$ condensates were recovered after photobleaching when compared with those of YFP-PodJ$_{CC1-3}$ and YFP-PodJ$_{IDR}$ in *E. coli*. White arrow, the photobleached region. Scale bar, 1 µm. **b**, Quantitative analysis of FRAP in panel a. The FRAP recovery curves were generated by averaging the signals of YFP-PodJ or its variants (n = 4 cells in YFP-PodJ$_{CC4-6}$; n = 8 cells in other samples) from at least two independent experiments with nonlinear regression. The fluorescence intensity of the pre-bleached region was normalized as 100%. Data are means ± SEM and p value was determined by one-way ANOVA. Source data are provided in the Source Data file.

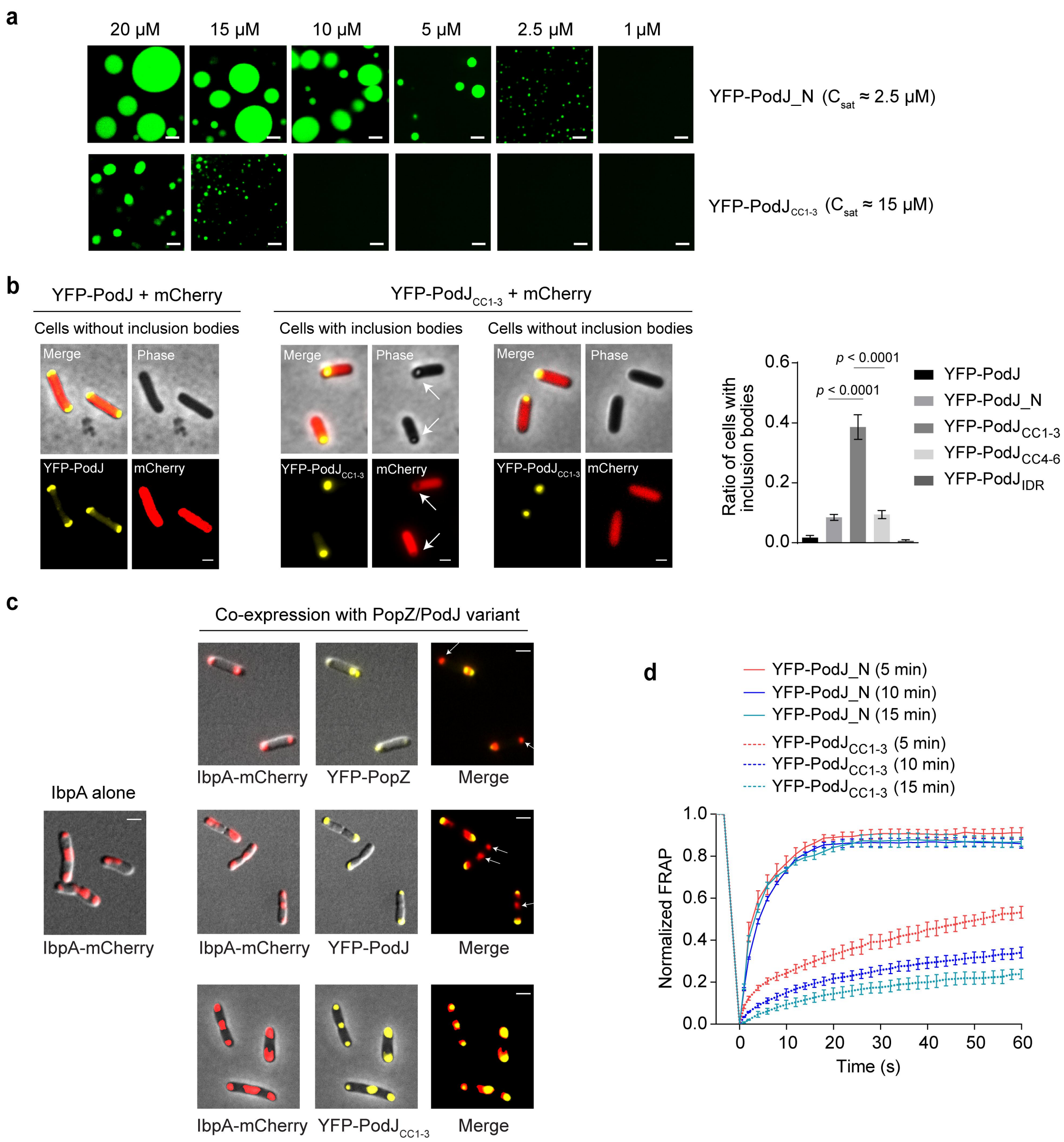

Supplementary Figure 5. CC1-3 phase separates at a higher concentration in vitro and forms insoluble aggregates in *E. coli*. a, YFP-PodJ$_{CC1\text{-}3}$ forms liquid droplets in vitro with a C_{sat} of ~15 μM. Images were taken within 15 min after loading the ice-bathed proteins (1, 2.5, 5, 10, 15 or 20 μM) on a glass pad at 25 °C. C_{sat}, protein concentration of saturation for LLPS. Scale bar, 5 μm. **b**, PodJ$_{CC1\text{-}3}$ forms a large number of insoluble aggregates in *E. coli*. Co-expression assay shows that YFP-PodJ$_{CC1\text{-}3}$ tends not to let mCherry enter the polar clusters, in contrast to the full-length YFP-PodJ. White arrows indicate the insoluble aggregates of YFP-PodJ$_{CC1-3}$. The percentages of cells with insoluble aggregates were calculated in each sample (*n* = 250, 300, 450, 350, and 250 cells; from top to bottom) from at least five independent experiments. Data are means ± SEM and *p* value was determined by one-way ANOVA. Scale bar, 1 µm. **c**, PodJ$_{CC1-3}$ co-localizes with IbpA while PodJ and PopZ do not co-localize with IbpA in *E. coli*. Co-expression of YFP-PodJ$_{CC1-3}$ and inclusion body marker protein A[4] (IbpA-mCherry) in *E. coli* showed co-localization of them, indicating that PodJ$_{CC1-3}$ forms inclusion bodies. In contrast, co-expression of YFP-PodJ/PopZ and IbpA-mCherry showed non-colocalization of these proteins, indicating that PodJ/PopZ does not form inclusion bodies. White arrows indicate the non-colocalization of proteins. Scale bar, 1 µm. **d**, PodJ$_{CC1-3}$ droplet ages over time. FRAP analyses were performed for YFP-PodJ$_{CC1-3}$ and YFP-PodJ_N droplets at different time points (5, 10 or 15 min) after loading the ice-bathed proteins (20 µM) on a glass pad at 25 °C. The recovery curves for each sample were generated by averaging the signals of droplets (*n* = 6) from three independent experiments. Data are means ± SEM. The results show that PodJ$_{CC1-3}$ droplets become less dynamic over time in contrast to PodJ_N droplets, a phenotype of protein aging that has been described previously in phase-separating proteins[5]. Source data are provided in the Source Data file.

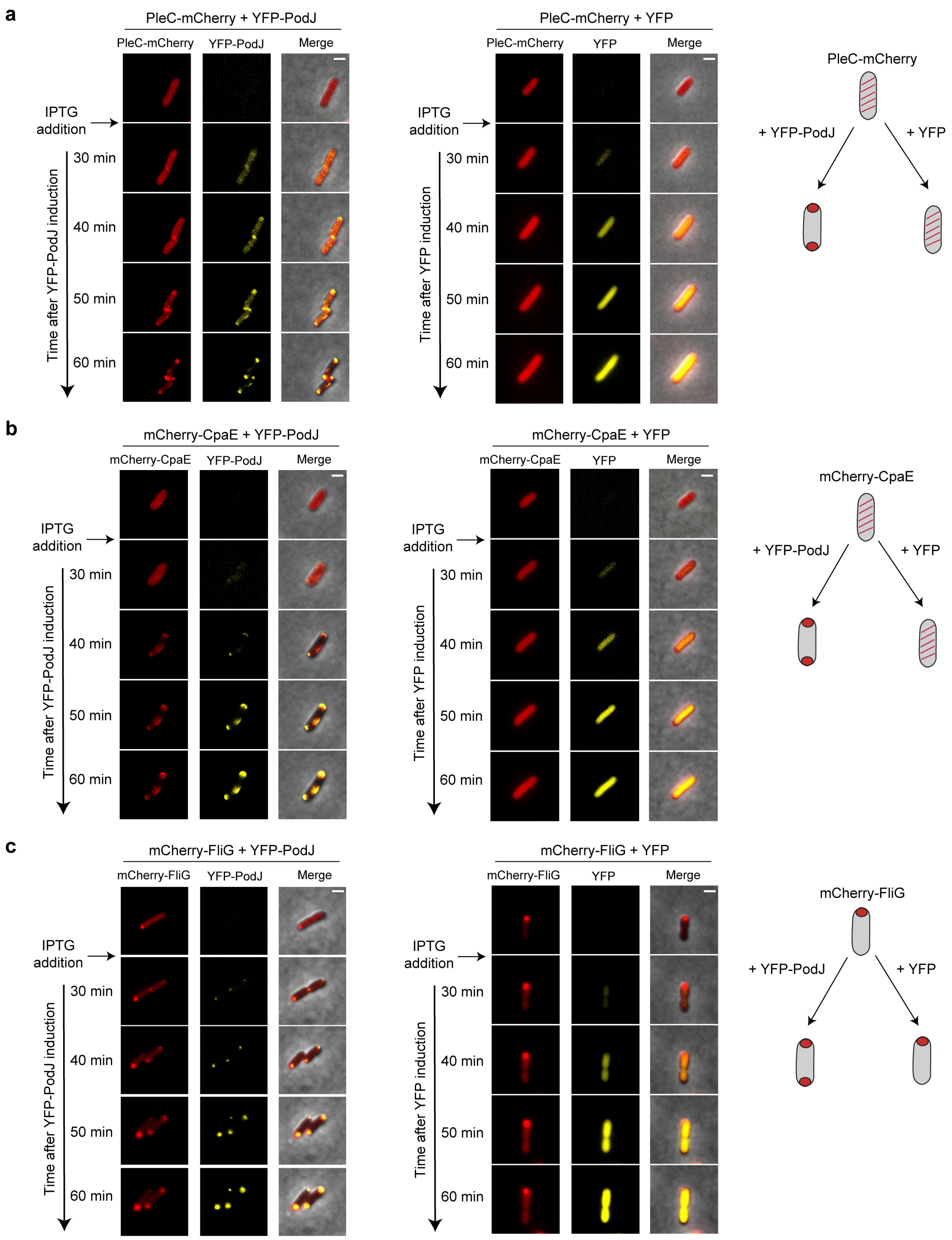

Supplementary Figure 6. Live cell imaging shows that PodJ recruits the client proteins in *E. coli*. The clients, including PleC (**a**), CpaE (**b**), and FliG (**c**) were pre-induced by 5 mM L-arabinose in *E. coli*, and their changes in subcellular localizations were recorded after the addition of 0.5 mM IPTG (PodJ induction). Images were acquired every 5 min on a LB pad at 37 °C. YFP was used as the negative controls in the middle panels. Schematic diagrams are presented as the right panels illustrating the changes in subcellular localizations of the three client proteins after induction of YFP-PodJ or YFP. All scale bars, 2 μm.

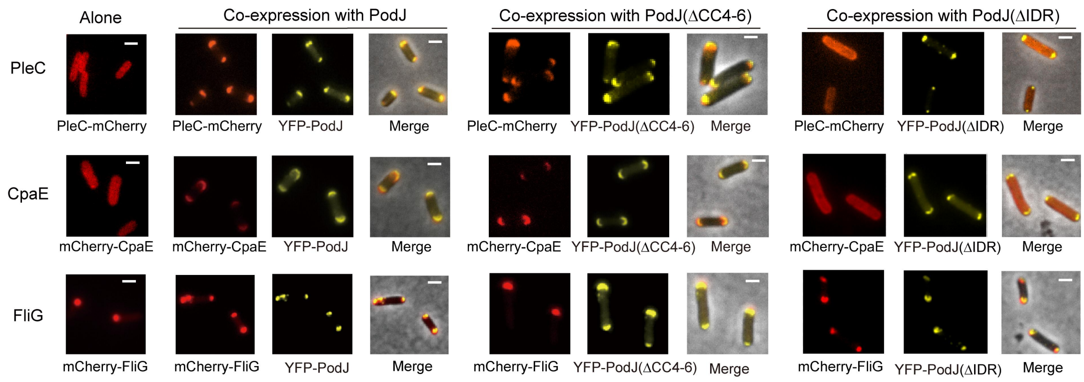

Supplementary Figure 7. Identification of the domains for client recruitment in PodJ by heterologous co-expression experiments. The client proteins, including PleC, CpaE, and FliG, were expressed alone or co-expressed with PodJ or PodJ variants in *E. coli* to observe their changes of subcellular localization. Quantitative results (see Fig. 4b) showed that IDR is responsible for the recruitment of PleC and CpaE, while CC4-6 is responsible for the interaction with FliG. Scale bar, 2 µm.

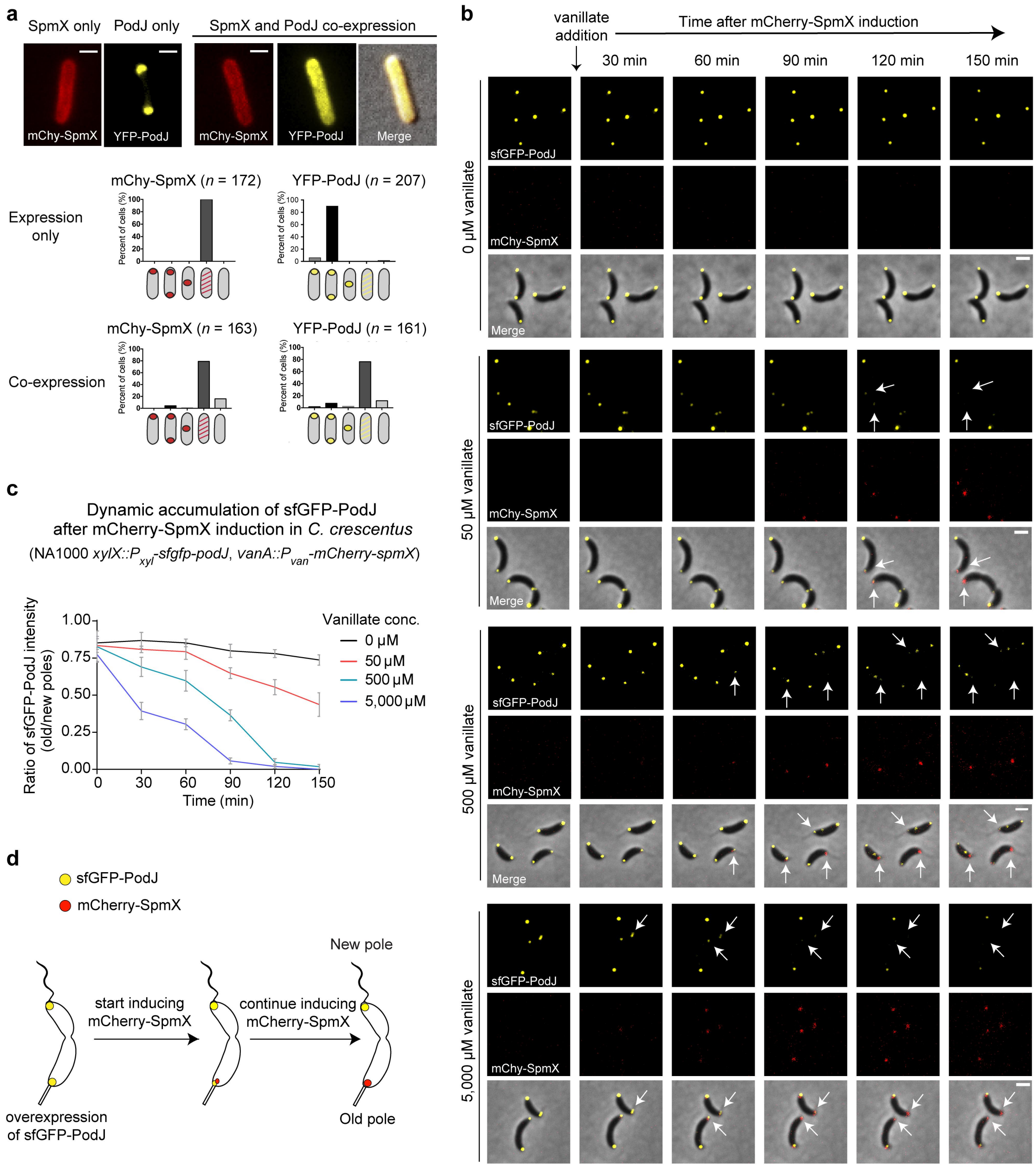

Supplementary Figure 8. SpmX regulates the dissociation of PodJ condensates in living cells. a, Overexpression of SpmX disrupts the polar accumulation of PodJ in *E. coli.* Co-expression of YFP-PodJ and mCherry-SpmX resulted in YFP-PodJ diffuse in *E. coli*. Histogram represents the percentage of cells with different protein localization patterns. Scale bar, 1 µm. **b**, Titration of sfGFP-PodJ with mCherry-SpmX reveals that SpmX regulates the disassembly of PodJ condensates at the cell poles of *C. crescentus*. Cells of the recombinant strain (NA1000, *xylX::P$_{xyl}$-sfgfp-podJ*, *vanA::P$_{van}$-mCherry-spmX*) were first induced with 0.03% (w/v) xylose for 3 h to create the bipolar model of sfGFP-PodJ. The cells were then immobilized on a 1.5% (w/v) agarose-PYE pad containing 0.03% (w/v) xylose and different concentrations of vanillate (0, 50, 500, or 5,000 μM, for mCherry-SpmX titration). Images were acquired every 5 min at 30 °C. The fluorescence intensities of sfGFP-PodJ at both cell poles were recorded. White arrows indicate the dissociation of sfGFP-PodJ at the old cell poles. Scale bar, 2 μm. **c**, The ratio of sfGFP-PodJ intensities (old to new poles) were generated by averaging signals of sfGFP-PodJ foci (*n* = 21 cells) from three independent experiments in panel b. Data are means ± SEM. **d**, Schematic diagram illustrating the changes in subcellular localizations of sfGFP-PodJ after induction of mCherry-SpmX in *C. crescentus*. The results showed that the dissociation of sfGFP-PodJ at the cell poles (especially at the old cell pole) by mCherry-SpmX was in a concentration-dependent manner. Source data are provided in the Source Data file.

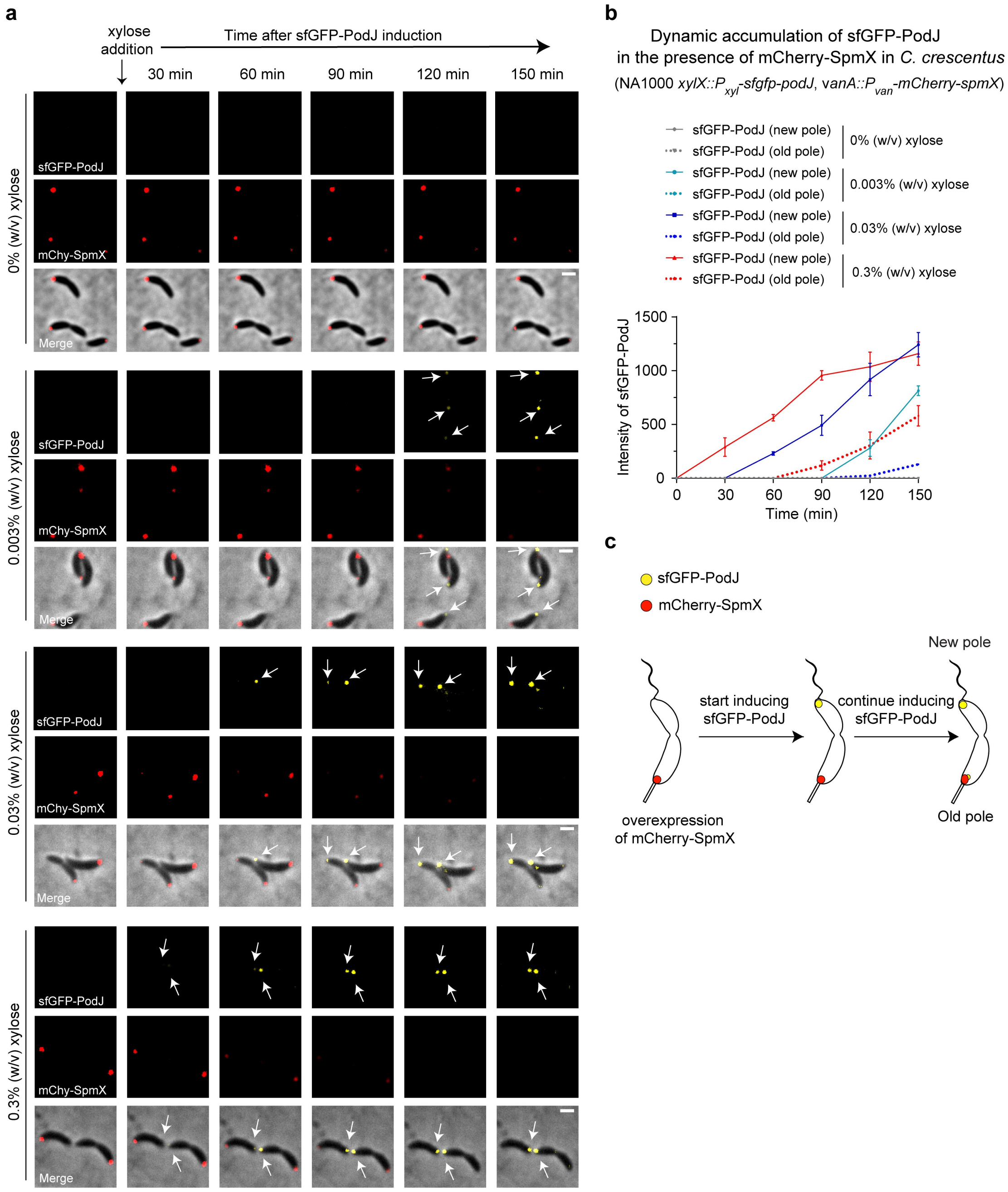

Supplementary Figure 9. SpmX regulates the subcellular formation of PodJ condensates in *C. crescentus*. a, Titration of mCherry-SpmX with sfGFP-PodJ reveals that SpmX regulates the formation of PodJ condensates at the cell poles of *C. crescentus*. Cells of the recombinant strain (NA1000, *xylX::P$_{xyl}$-sfgfp-podJ*, *vanA::P$_{van}$-mCherry-spmX*) were first induced with 50 µM vanillate for 3 h to create the monopolar model of mCherry-SpmX. The cells were then immobilized on a 1.5%

(w/v) agarose-PYE pad containing 50 μM vanillate and different concentrations of xylose (0, 0.003%, 0.03%, or 0.3% (w/v), for sfGFP-PodJ titration). Images were acquired every 5 min at 30 °C. The fluorescence intensities of sfGFP-PodJ at both cell poles were recorded. White arrows indicate the formation of sfGFP-PodJ condensates at the new cell poles. Scale bar, 2 μm. **b**, The sfGFP-PodJ intensities at both cell poles (old and new poles) were calculated by averaging signals of sfGFP-PodJ foci (n = 21 cells) from three independent experiments in panel a. Data are means ± SEM. **c**, Schematic diagram illustrating the changes in subcellular localizations of sfGFP-PodJ in the presence of mCherry-SpmX in *C. crescentus*. The results showed that sfGFP-PodJ preferred to accumulate at the new cell pole. Source data are provided in the Source Data file.

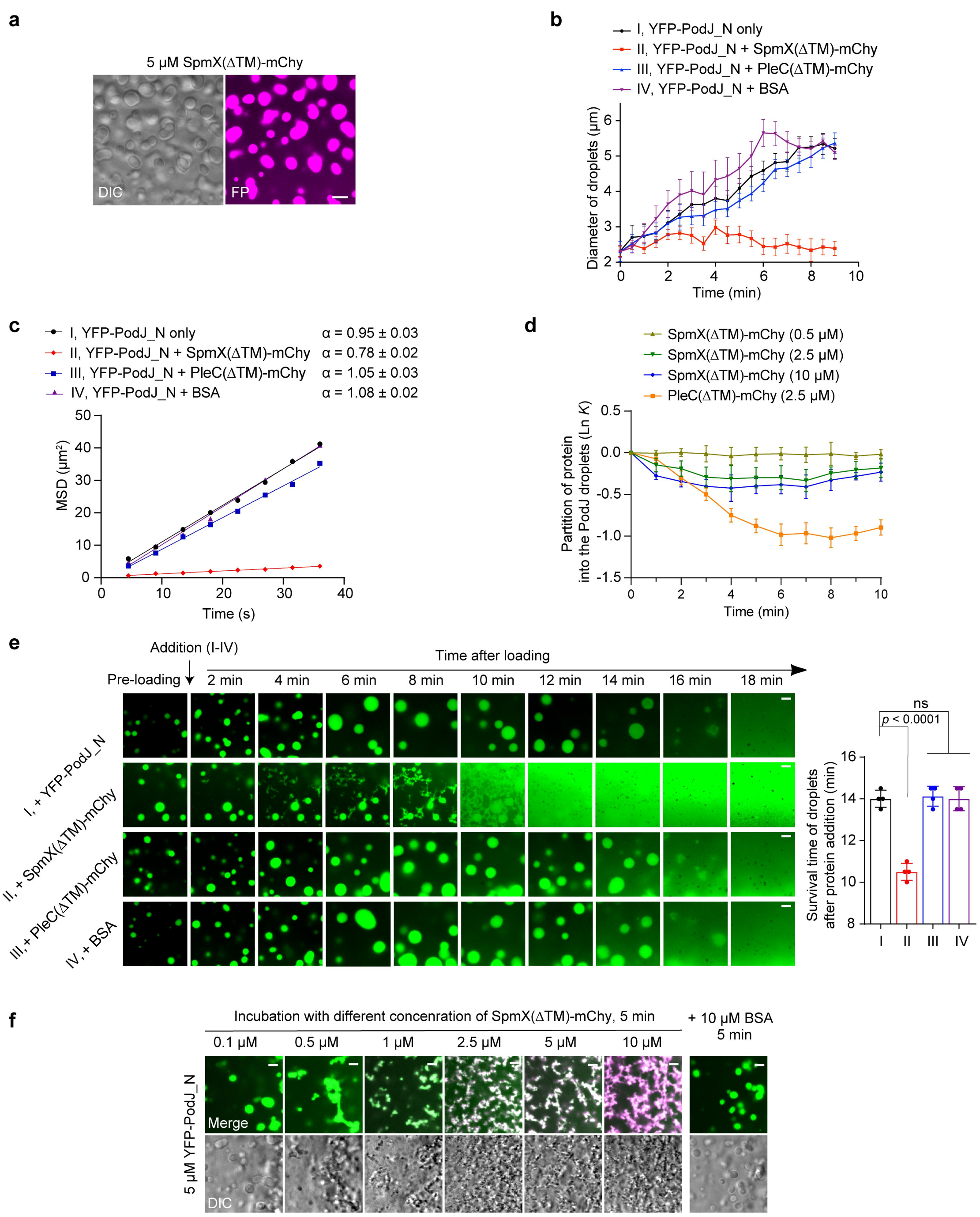

Supplementary Figure 10. SpmX negatively regulates PodJ LLPS in vitro. a, SpmX(ΔTM)-mCherry (5 μM) forms clear liquid droplets in vitro at 25 °C. **b**, The YFP-PodJ_N droplets were unable to grow in the presence of SpmX(ΔTM)-mCherry. Diameter analysis was performed by measurements of droplets from three independent experiments in each sample (*n* = 1,982, 1,540, 1,112, and 786 droplets;

from top to bottom). Data are means ± SEM. **c**, The motility analyses of YFP-PodJ_N droplets by tracking single microspheres. Droplets (*n* = 24, 25, 25, and 25 droplets; from top to bottom) from three independent experiments were analyzed, respectively. Mean-square displacement (MSD) versus time was measured for YFP-PodJ_N droplets in the presence of SpmX(ΔTM)-mCherry or PleC(ΔTM)-mCherry, using the addition of BSA as the control. The anomalous diffusion exponent (α) was obtained by fitting the dataset with log(MSD(t)) and t, where the slope of the linear fit is α. The average MSD increased non-linearly ($\alpha \approx 0.78$) for YFP-PodJ_N droplets in the presence of SpmX(ΔTM)-mCherry, showing sub-diffusion behavior. Corresponding to Fig. 5f. **d**, The partitioning analysis of SpmX(ΔTM)-mCherry into YFP-PodJ_N droplets. The solution of pre-formed YFP-PodJ_N (5 µM) droplets was mixed with 0.5, 2.5, or 10 µM SpmX(ΔTM)-mCherry. The 2.5 µM of PleC(ΔTM)-mCherry was used as the positive control. Droplets (*n* = 6) in each sample were analyzed from three independent experiments. Data are means ± SEM. The results show that SpmX did not mix with the formed PodJ droplets over time except for a very small portion of SpmX that penetrated into the droplets at the beginning, possibly before the interfacial interaction was completed. **e**, SpmX accelerates the disassembly of PodJ droplets in vitro. The solution of pre-formed YFP-PodJ_N (5 µM) droplets was mixed with 2.5 µM SpmX(ΔTM)-mCherry or PleC(ΔTM)-mCherry, using the addition of BSA as the control. Representative images are shown on the left panel. The survival time of YFP-PodJ_N droplets (*n* = 100) in each sample were recorded and analyzed after protein addition from four independent experiments (right panel). Data are means ± SEM and *p* value was determined by one-way ANOVA. ns, non-significant. **f**, YFP-PodJ_N results in no droplets when incubated with as low as 0.5 μM SpmX(ΔTM)-mCherry. In vitro LLPS experiments were performed by incubating YFP-PodJ_N with different concentrations of SpmX(ΔTM)-mCherry (0.1, 0.5, 1, 2.5, 5, and 10 μM). Images were acquired after 5 min of incubation. All scale bars, 5 μm. Source data are provided in the Source Data file.

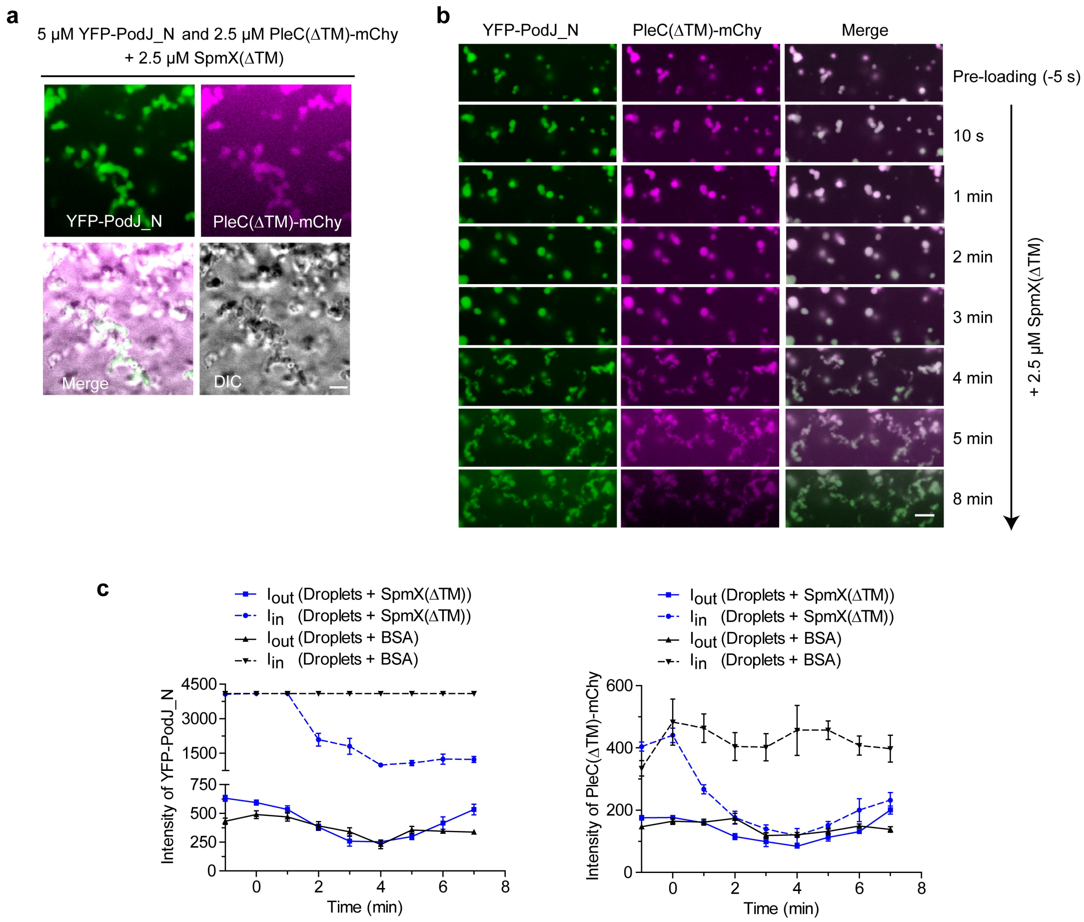

Supplementary Figure 11. The negative regulation of PodJ by SpmX for client recruitment. a, Incubation with SpmX(ΔTM) causes amorphous structures of YFP-PodJ_N and PleC(ΔTM)-mCherry. 5 µM YFP-PodJ_N and 2.5 µM PleC(ΔTM)-mCherry were incubated together with 2.5 µM SpmX(ΔTM)-mCherry for 15 min before imaging. **b**, The droplets of YFP-PodJ_N and PleC(ΔTM)-mCherry lose fluidity and produce amorphous structures after loading of SpmX(ΔTM). **c**, Intensity analysis of the droplets of YFP-PodJ_N and PleC(ΔTM)-mCherry with incubation of SpmX(ΔTM). Corresponding to Fig. 5j. 5 µM YFP-PodJ_N and 5 µM PleC(ΔTM)-mCherry were incubated for 15 min. Then, 2.5 µM SpmX(ΔTM) was added and images were acquired after another 5 min. The addition of 2.5 µM BSA was used as the control. The fluorescence intensities outside (I_{out}) and inside (I_{in}) the droplets were measured using Fiji/ImageJ. Droplets (n = 6) in each sample were measured from three independent experiments. Data are means ± SEM. All scale bars, 5 µm. Source data are provided in the Source Data file.

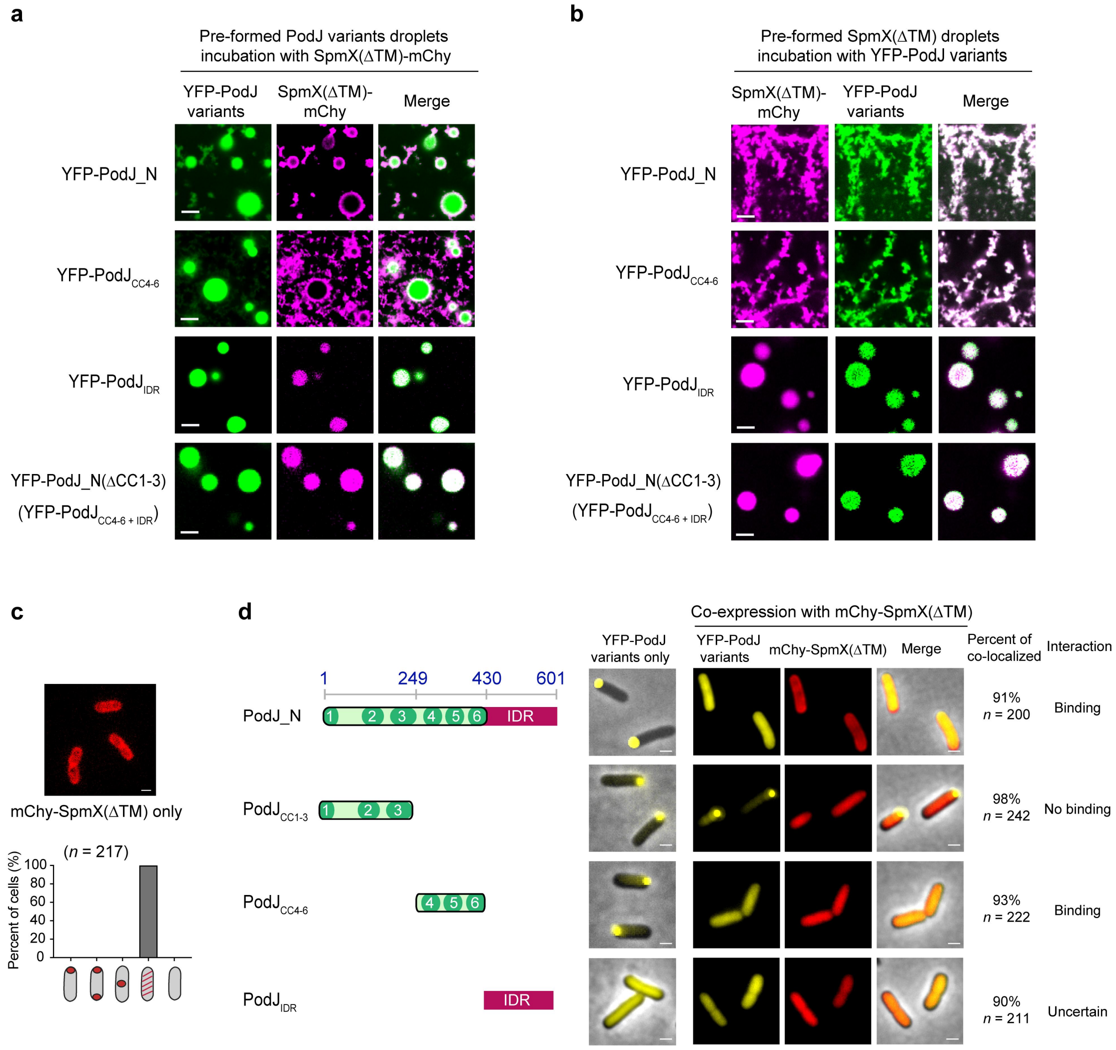

Supplementary Figure 12. CC4-6 is one of the interaction domains between PodJ and SpmX. a, SpmX(ΔTM) binds to the surface of $\text{PodJ}_{\text{CC4-6}}$ droplets but fuses together with PodJ_{IDR}. SpmX(ΔTM) interaction with $\text{PodJ}_{\text{CC4-6+IDR}}$ follows the same fusion pattern as that of SpmX(ΔTM) and PodJ_{IDR}. The pre-formed droplets of YFP-PodJ_N or its variants (5 μM) were incubated with 2.5 μM SpmX(ΔTM)-mCherry at 25 °C for 5 min before imaging. Scale bar, 5 μm. **b**, $\text{PodJ}_{\text{CC4-6}}$ interaction with the pre-formed SpmX(ΔTM) generates amorphous structures as that of PodJ_N. The pre-formed droplets of SpmX(ΔTM)-mCherry (5 μM) were incubated with 2.5 μM YFP-

PodJ_N and its variants at 25 °C for 5 min before imaging. Scale bar, 5 μm. **c**, mCherry-SpmX(ΔTM) expression alone is diffuse in *E. coli*. Histogram represents the percentage of cells with different protein localization patterns. Scale bar, 1 μm. **d**, Co-expression analyses of PodJ variants with SpmX(ΔTM) in *E. coli* show that CC4-6 is the interaction domain in PodJ. Representative images of cells co-expressed YFP-PodJ variants and mCherry-SpmX(ΔTM) are shown. Scale bar, 1 μm.

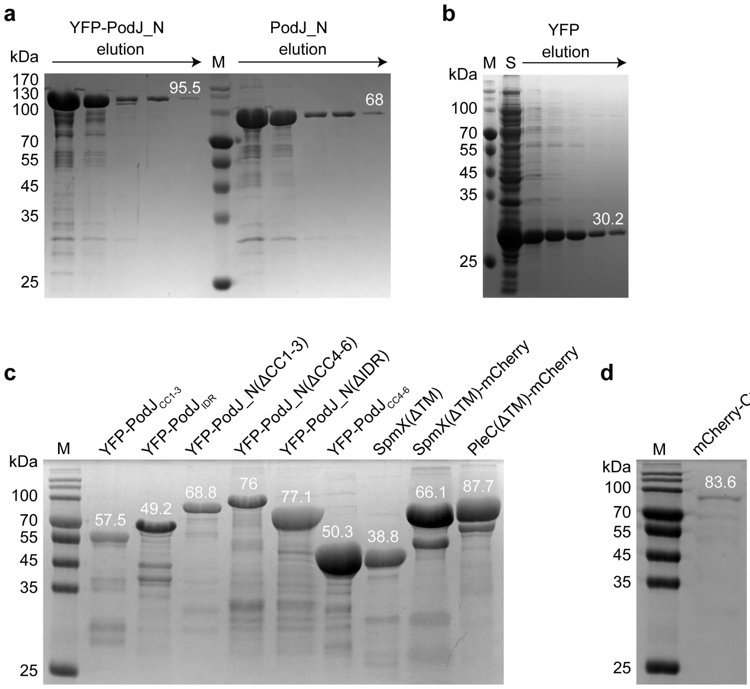

Supplementary Figure 13. SDS-PAGE analyses of the proteins used in this study.

The molecular masses predicted for each protein are shown on PAGE. **a,** YFP-PodJ_N and PodJ_N. **b,** YFP. **c,** YFP-PodJ variants, SpmX(ΔTM), SpmX(ΔTM)-mCherry and PleC(ΔTM)-mCherry. **d,** mCherry-CpaE. M, protein marker. S, supernatant. All the proteins were collected with purity > 80% and were stored at -80 °C before use. Concentrations of purified proteins were determined using a Bradford protein assay kit. Source data are provided in the Source Data file.

Supplementary tables

Supplementary Table 1. Screening of PodJ client proteins in *E. coli*.

Locus tag	Protein	Predicted function	Observed localization		Co-localization relationship
			Expression alone	Co-expression with YFP/CFP-PodJ[a]	
CCNA_00268	DnaX	DNA polymerase III subunit gamma/tau	Monopolar	Monopolar	No co-localization
CCNA_00437	McpB	Methyl-accepting chemotaxis protein	Diffuse	Diffuse	No co-localization
CCNA_00441	CheYI	Chemotaxis receiver domain protein	Diffuse	Diffuse	No co-localization
CCNA_00442	CheAI	Chemotaxis histidine kinase protein	Diffuse	Diffuse	No co-localization
CCNA_00538		Methyl-accepting chemotaxis protein	Bipolar	Bipolar	Uncertain
CCNA_00947	FlgE	Flagellar hook protein	Diffuse	Diffuse	No co-localization
CCNA_00950	FliF	Flagellar M-ring protein	Diffuse	Diffuse	No co-localization
CCNA_00951	FliG	Flagellar motor switch protein	Monopolar	Bipolar	Co-localized
CCNA_01132	CckA	Sensory transduction histidine kinase/receiver	Diffuse	Diffuse	No co-localization
CCNA_01528	FljK	Flagellin	Monopolar	Monopolar	No co-localization
CCNA_01918	PopA	Cyclic di-GMP effector protein	Diffuse	Bipolar	Co-localized
CCNA_02546	PleD	GGDEF/response regulator protein	Diffuse	Diffuse	No co-localization

CCNA_02547	DivK	Response regulator receiver protein	Diffuse	Diffuse	No co-localization
CCNA_02567	PleC	Sensory transduction histidine kinase	Diffuse	Bipolar	Co-localized
CCNA_02623	FtsZ	Cell division protein	Patching	Patching	Uncertain
CCNA_02643	FtsI	Penicillin-binding protein	Monopolar	Monopolar	No co-localization
CCNA_03037	CpaF	Pilus assembly ATPase	Monopolar	Monopolar	No co-localization
CCNA_03038	CpaE	Pilus assembly ATPase	Diffuse	Bipolar	Co-localized
CCNA_03039	CpaD	Pilus assembly protein	Diffuse	Diffuse	No co-localization
CCNA_03043	PilA	Type IV pilin protein	Diffuse	Diffuse	No co-localization
CCNA_03598	DivL	Two-component sensor histidine kinase	Diffuse	Diffuse	No co-localization
CCNA_03868	ParB	Chromosome partitioning protein	Diffuse	Diffuse	No co-localization
CCNA_03869	ParA	Chromosome partitioning protein	Diffuse	Diffuse	No co-localization

[a]YFP/CFP-PodJ expression alone and co-expression with potential client proteins were in a bipolar pattern in *E. coli*.

Supplementary Table 2. Screening of the regulators of PodJ subcellular localization in *E. coli*.

Locus tag	Protein	Predicted function	Observed localization		Observed PodJ localization[a] (co-expressed)
			Expression alone	Co-expression with YFP/CFP-PodJ[a]	
CCNA_00439	McpA	Methyl-accepting chemotaxis protein	Diffuse	Diffuse	Bipolar
CCNA_00803	CheW	Chemotaxis protein	Diffuse	Diffuse	Bipolar
CCNA_01755		Two component sensor histidine kinase	Bipolar	Bipolar	Bipolar
CCNA_01815	NtrC	Nitrogen assimilation regulatory protein	Diffuse	Diffuse	Bipolar
CCNA_01817	NtrX	Nitrogen assimilation regulatory protein	Diffuse	Diffuse	Bipolar
CCNA_01926	DgcB	GGDEF diguanylate cyclase	Diffuse	Diffuse	Bipolar
CCNA_02255	SpmX	Lysozyme-family localization factor	Diffuse	Diffuse	Diffuse
CCNA_03281		AsnC-family transcriptional regulator	Diffuse	Diffuse	Bipolar
CCNA_03333		PAS-family sensor histidine kinase	Diffuse	Diffuse	Bipolar
CCNA_03424	TacA	AAA-family response regulator	Monopolar	Monopolar	Bipolar
CCNA_03584	ChpT	Histidine phosphotransferase	Diffuse	Diffuse	Bipolar

[a]YFP/CFP-PodJ was expressed alone in *E. coli* cells in a bipolar pattern.

Supplementary Table 3. Bacterial strains used in this study.

Strains	Description[a]	Reference/Source
C. crescentus		
NA1000	*C. crescentus* wild-type strain	Lucy Shapiro lab
LS3778	*C. crescentus* NA1000 Δ*podJ*	ref[6]
GB255	*C. crescentus* NA1000 Δ*popZ*	ref[7]
LS4367	*C. crescentus* NA1000 Δ*tipN*	ref[8]
SKR265	*C. crescentus* NA1000 Δ*spmX*	ref[9]
WTS199	Kan^R; *C. crescentus* NA1000 Δ*podJ*, *xylX::*P_{xyl}*-sfgfp-podJ*	This study
WTS230	Chl^R; *C. crescentus* NA1000, *pBVMCS6-*P_{van}*-pleC-mCherry*	This study
WTS231	Chl^R; *C. crescentus* NA1000 Δ*podJ*, *pBVMCS6-*P_{van}*-pleC-mCherry*	This study
WTS263	Kan^R; *C. crescentus* NA1000, *pBXMCS2-*P_{xyl}*-yfp-podJ_N*	This study
WTS265	Kan^R; *C. crescentus* NA1000 Δ*spmX*, *pBXMCS2-*P_{xyl}*-yfp-podJ_N*	This study
WTS210	Kan^R; *C. crescentus* NA1000 Δ*popZ*, *xylX::*P_{xyl}*-sfgfp-podJ*	This study
WTS345	Kan^R; *C. crescentus* NA1000 Δ*tipN*, *xylX::*P_{xyl}*-sfgfp-podJ*	This study
WTS211	Kan^R; *C. crescentus* NA1000 Δ*spmX*, *xylX::*P_{xyl}*-sfgfp-podJ*	This study
WTS158	Kan^R; *C. crescentus* NA1000, *xylX::*P_{xyl}*-sfgfp-podJ*	This study
WTS115	Kan^R; *C. crescentus* NA1000, *xylX::*P_{xyl}*-podJ*	This study
WTS296	Kan^R; *C. crescentus* NA1000, *xylX::pXYFPN2-*P_{xyl}	This study

WTS179	Kan^R, Chl^R; *C. crescentus* NA1000, *xylX::*P_{xyl}*-sfgfp-podJ*, *pBVMCS6-*P_{van}*-mCherry-spmX*	This study
WTS239	Chl^R; *C. crescentus* NA1000, *pBVMCS6-*P_{van}*-mCherry-cpaE*	This study
WTS240	Chl^R; *C. crescentus* NA1000 Δ*podJ*, *pBVMCS6-*P_{van}*-mCherry-cpaE*	This study
WTS241	Kan^R, Chl^R; *C. crescentus* NA1000 Δ*podJ*, *xylX::*P_{xyl}*-sfgfp-podJ*, *pBVMCS6-*P_{van}*-mCherry-cpaE*	This study
WTS270	Chl^R; *C. crescentus* NA1000, *pBVMCS6-*P_{van}*-mCherry-fliG*	This study
WTS271	Chl^R; *C. crescentus* NA1000 Δ*podJ*, *pBVMCS6-*P_{van}*-mCherry-fliG*	This study
WTS285	Kan^R, Chl^R; *C. crescentus* NA1000 Δ*podJ*, *xylX::*P_{xyl}*-sfgfp-podJ*, *pBVMCS6-*P_{van}*-mCherry-fliG*	This study
WTS202	Kan^R; *C. crescentus* NA1000 Δ*podJ*, *xylX::*P_{xyl}*-sfgfp-podJ_N*	This study
WTS232	Kan^R, Chl^R; *C. crescentus* NA1000 Δ*podJ*, *xylX::*P_{xyl}*-sfgfp-podJ*, *pBVMCS-6-*P_{van}*-pleC-mCherry*	This study
WTS275	Kan^R, Chl^R; *C. crescentus* NA1000 Δ*podJ*, *xylX::*P_{xyl}*-sfgfp-podJ_N*, *pBVMCS6-*P_{van}*-pleC-mCherry*	This study
WTS342	Kan^R, Chl^R; *C. crescentus* NA1000 *xylX::*P_{xyl}*-sfgfp-podJ*, *vanA::*P_{van}*-mCherry-spmX*	This study
E. coli		
DH5α	Bacterial cloning strain	Novagen
BL21(DE3)	Bacterial expression strain	Novagen

[a]Abbreviations: Kan, kanamycin; Chl, Chloramphenicol; R, resistance.

Supplementary Table 4. Plasmids used in this study.

Plasmid	Plasmid information[a]	Reference/Source
pWT188	Kan^R; pBXMCS2-P_{xyl}-mNG-PodJ	This study
pWT022	Kan^R; pXYFPN2-P_{xyl}-sfGFP-PodJ	This study
pWT194	Chl^R; pBVMCS6-P_{van}-PleC-mCherry	This study
pWT191	Chl^R; pBVMCS6-P_{van}-mCherry-SpmX	This study
pWT205	Kan^R; pBXMCS2-P_{xyl}-YFP-PodJ	This study
pWT206	Kan^R; pBXMCS2-P_{xyl}-YFP-PodJ_N	This study
pWT195	Chl^R; pBVMCS6-P_{van}-mCherry-CpaE	This study
pWT200	Chl^R; pBVMCS6-P_{van}-mCherry-FliG	This study
pWT147	Kan^R; pXYFPN2-P_{xyl}-sfGFP-PodJ_N	This study
pWT243	Chl^R; pVCHYN6-P_{van}-mCherry-SpmX	This study
pWT046	Kan^R; pXYFPN2-P_{xyl}-PodJ	This study
pWT212	Kan^R; pXYFPN2-P_{xyl}	This study
pWT011	$Spec^R$; pCDF-YFP-PodJ	This study
pWT038	Amp^R; pBAD-CFP-PodJ	This study
pWT009	Chl^R; pACYC-mCherry-CpaE	This study
pWT244	$Spec^R$; pCDF-IbpA-mCherry	This study
pWT245	Amp^R; pBAD-YFP-PodJ	This study

pWT246	Amp^R; pBAD-YFP-$PodJ_{CC1-3}$	This study
pWT015	Chl^R; pACYC-FtsZ-mCherry	This study
pWT247	Amp^R; pBAD-CckA-mCherry	This study
pWT248	Amp^R; pBAD-DivK-mCherry	This study
pWT249	Amp^R; pBAD-DivL-mCherry	This study
pWT250	Chl^R; pACYC-PleD-mCherry	This study
pWT014	Chl^R; pACYC-PopA-mCherry	This study
pWT080	Amp^R; pBAD-PleC-mCherry	This study
pWT081	Amp^R; pBAD-mCherry-PopZ	This study
pWT251	$Spec^R$; pCDF-mCherry-PopZ	This study
pWT013	Chl^R; pACYC-mCherry-SpmX	This study
pWT012	Amp^R; pBAD-SpmX(ΔTM)-mCherry	This study
pWT252	Chl^R; pACYC-CFP-ParB	This study
pWT253	Chl^R; pACYC-ParA-mCherry	This study
pWT207	Amp^R; pBAD-YFP-PopZ	This study
pWT003	$Spec^R$; pCDF-YFP-$PodJ_{CC1-3}$	This study
pWT082	$Spec^R$; pCDF-YFP	This study
pWT174	$Spec^R$; pCDF-YFP-$PodJ_{CC4-6}$	This study
pWT173	$Spec^R$; pCDF-YFP-$PodJ_{IDR}$	This study
pWT079	$Spec^R$; pCDF-YFP-PodJ_N	This study

pWT165	$Spec^R$; pCDF-YFP-PodJ(ΔIDR)	This study
pWT024	$Spec^R$; pCDF-YFP-PodJ(ΔCC4-6)	This study
pWT004	Amp^R; pBAD-mCherry-$SpmX_{1-356}$	This study
pWT005	Amp^R; pBAD-PopA-mCherry	This study
pWT006	Amp^R; pBAD-FtsZ-mCherry	This study
pWT007	Amp^R; pBAD-mCherry-CpaE	This study
pWT027	Amp^R; pBAD-FljK-mCherry	This study
pWT028	Amp^R; pBAD-FlgE-mCherry	This study
pWT029	Amp^R; pBAD-CpaF-mCherry	This study
pWT030	Amp^R; pBAD-PilA-mCherry	This study
pWT031	Amp^R; pBAD-McpA-mCherry	This study
pWT032	Amp^R; pBAD-McpB-mCherry	This study
pWT033	Amp^R; pBAD-CheAI-mCherry	This study
pWT034	Amp^R; pBAD-CheYI-mCherry	This study
pWT057	Amp^R; pBAD-mCherry-FliF	This study
pWT059	Amp^R; pBAD-mCherry-CCNA_03333	This study
pWT060	Amp^R; pBAD-mCherry-ChpT	This study
pWT061	Amp^R; pBAD-mCherry-FtsI	This study
pWT062	Amp^R; pBAD-mCherry-CCNA_00538	This study
pWT063	Amp^R; pBAD-CheW-mCherry	This study

pWT064	Amp^R; pBAD-FliF-mCherry	This study
pWT025	Amp^R; pBAD-mCherry-FliG	This study
pWT066	Amp^R; pBAD-CCNA_01755-mCherry	This study
pWT067	Amp^R; pBAD-NtrC-mCherry	This study
pWT068	Amp^R; pBAD-NtrX-mCherry	This study
pWT069	Amp^R; pBAD-DgcB-mCherry	This study
pWT070	Amp^R; pBAD-CpaD-mCherry	This study
pWT071	Amp^R; pBAD-CCNA_03281-mCherry	This study
pWT072	Amp^R; pBAD-TacA-mCherry	This study
pWT073	Amp^R; pBAD-DnaX-mCherry	This study
pWT076	Amp^R; pBAD-CCNA_00538-mCherry	This study
pWT240	Amp^R; pBAD-mCherry	This study
pWT001	Amp^R; pTEV5-PodJ_N	This study
pWT086	Amp^R; pTEV5-YFP-PodJ_N(ΔCC1-3)	This study
pWT037	Amp^R; pTEV5-YFP-PodJ_N	This study
pWT039	Amp^R; pTEV5-YFP	This study
pWT170	Amp^R; pTEV5-YFP-PodJ_N(ΔIDR)	This study
pWT141	Amp^R; pTEV5-YFP-$PodJ_{CC1-3}$	This study
pWT142	Amp^R; pTEV5-YFP-$PodJ_{CC4-6}$	This study
pWT144	Amp^R; pTEV5-YFP-$PodJ_{IDR}$	This study

pWT146	Amp^R; pTEV5-YFP-PodJ_N(ΔCC4-6)	This study
pET28a(+)	Kan^R; bacterial protein expression vector	Novagen
pWT150	Kan^R; pET28a-mCherry-SpmX(ΔTM)	This study
pWT154	Kan^R; pET28a-mCherry-CpaE	This study
pWT156	Kan^R; pET28a-PleC-mCherry	This study
pWT169	Kan^R; pET28a-PleC(ΔTM)-mCherry	This study
pWT187	Kan^R; pET28a-mCherry-PopZ	This study
pWT189	Kan^R; pET28a-SpmX(ΔTM)	This study
pWT190	Kan^R; pET28a-SpmX(ΔTM)-mCherry	This study
pWT209	Kan^R; pET28a-mCherry	This study

[a]Abbreviations: Kan, kanamycin; Chl, chloramphenicol; Spec, spectinomycin; Amp, ampicillin; R, resistance.

Supplementary Table 5. Oligonucleotides used in this study.

Primer	Sequence	Constructs
WTP139	gagacgaccatatgacggcggcttcgccatg	pWT046
WTP140	gccgccgtcatatggtcgtctccccaaaactc	
WTP602	gagacgaccatgccttaattaatatgcatgg	pWT212
WTP603	ttaaggcatggtcgtctccccaaaactcgagc	
WTP464	aggcaagggctaagccttaattaatatgca	pWT147
WTP465	ttaaggcttagcccttgccttccgaggcgg	
WTP528	gaactgtacaaataagccttaattaatatgca	pWT166
WTP529	ttaaggcttatttgtacagttcatccatac	
WTP548	ggatcagcgccaccggtcggccaccatgcgtaaaggcgaagagct	pWT180
WTP549	taattaaggcttatttgtacagttcatccatacca	
WTP550	gaactgtacaaataagccttaattaatatgcatggtaccttaagatct	
WTP551	ctttacgcatggtggccgaccggtggcgctgatccagggcctgga	
WTP007	ggatcagcgctaagcagatctcaattggat	pWT003
WTP008	gatctgcttagcgctgatccagggcctggaac	
WTP459	ggatcagcgccaggaactggtcgaccgcat	pWT024
WTP460	ccagttcctggcgctgatccagggcctggaac	
WTP137	aggagatataatgacggcggcttcgccatg	pWT045

WTP138	gccgccgtcattatatctccttcttatactt	
WTP147	aggcaagggctaattaacctaggctgctgc	pWT079 or pWT049
WTP148	aggttaattagcccttgccttccgaggcgg	
WTP254	gctgtacaagtaagcagatctcaattggat	pWT082
WTP255	gatctgcttacttgtacagctcgtccatgc	
WTP526	gaacgttccagctaagcagatctcaattggat	pWT164
WTP527	gatctgcttagctggaacgttcgtggcgtt	
WTP524	gaacgttccagcggcaaggccaagtcggcgaa	pWT165
WTP525	tggccttgccgctggaacgttcgtggcgtt	
WTP530	aggcaagggctaagcagatctcaattggata	pWT167
WTP531	gatctgcttagcccttgccttccgaggcggc	
WTP009	ggtggagccgtaagaagcttggctgttttggcggatgagagaagat	pWT004
WTP010	tgctcaccatttaattcctcctgttagcccaaaaaacgggtatggaga	
WTP011	gaggaattaaatggtgagcaagggcgaggag	
WTP012	aagcttcttacggctccaccagcggcac	
WTP013	cgctgaagcgcgaggcgggccaccggtcggccacc	pWT005
WTP014	attcgggcgtcaaccgccatttaattcctcctgttagcccaaaaaacgggtatgg	
WTP015	gggctaacaggaggaattaaatggcggttgacgcc	
WTP016	accatggtggccgaccggtggcccgcctcgcg	

WTP017	tcctgcgccgcctggccaaccaccggtcggccacc	pWT006
WTP018	gcggaaagagaaatagccatttaattcctcctgttagcccaaaaaacgg	
WTP019	gggctaacaggaggaattaaatggctatttctctttccgcg	
WTP020	accatggtggccgaccggtggttggccaggcg	
WTP021	gaagaagtaggaagcttggctgttttggcggatgagag	pWT007
WTP022	tgctcaccatttaattcctcctgttagcccaaaaaacgggtatggaga	
WTP023	gaggaattaaatggtgagcaagggcgaggag	
WTP024	gccaagcttcctacttcttcttgaacaggcccgagaaca	
WTP064	cctgttccgtcaccggtcggccaccatgg	pWT027
WTP065	tcagcgccatttaattcctcctgttagcccaaaaaacgggtatggagaaacagtagagag	
WTP066	gaggaattaaatggcgctgaacagcatcaatacgaacg	
WTP067	ccgaccggtgacggaacaggctcaggatcgagg	
WTP068	tattaagcgccaccggtcggccaccatgg	pWT028
WTP069	tgatgctcatttaattcctcctgttagcccaaaaaacgggtatggag	
WTP070	gaggaattaaatgagcatcaacagcgccatgct	
WTP071	ccgaccggtggcgcttaatattcaagagttcctcaagcatctggt	
WTP072	cgcggcggagcaccggtcggccaccatgg	
WTP073	ttccgaacatttaattcctcctgttagcccaaaaaacgggtatggag	
WTP074	gaggaattaaatgttcggaaagcgcgactcgt	

WTP075	ccgaccggtgctccgccgcgtcgaggg	pWT029
WTP076	ggctggcacccaccggtcggccaccatgg	pWT030
WTP077	acttggtcatttaattcctcctgttagcccaaaaaacgggtatggag	
WTP078	gaggaattaaatgaccaagttcgtcacgcgct	
WTP079	ccgaccggtgggtgccagccgccgt	
WTP080	ggaggaattccaccggtcggccaccatggtgag	pWT031
WTP081	tcgccaacatttaattcctcctgttagcccaaaaaacgggtatggag	
WTP082	gaggaattaaatgttggcgatccgtgggcac	
WTP083	ccgaccggtggaattcctcccaaccatccgaggcg	
WTP084	ggaagaattccaccggtcggccaccatgg	pWT032
WTP085	cggtccccatttaattcctcctgttagcccaaaaaacgggtatggag	
WTP086	gaggaattaaatggggaccgccatgaaccag	
WTP087	ccgaccggtggaattcttcccactcttccttgaccgcgaccg	
WTP088	cgcagcggagcaccggtcggccaccatgg	pWT033
WTP089	gctcgtccatttaattcctcctgttagcccaaaaaacgggtatggagaaacagtagagag	
WTP090	gaggaattaaatggacgagctagaggccatcaaggtcaccttct	
WTP091	ccgaccggtgctccgctgcgatcaggctgg	
WTP092	cgtcgccgcccaccggtcggccaccatgg	pWT034
WTP093	tacgcgtcacttaattcctcctgttagcccaaaaaacgggtatggaga	

WTP094	gaggaattaagtgacgcgtacggttctcacggt	
WTP095	ccgaccggtgggcggcgacgcggcgga	
WTP164	cgagtcgacctaagaagcttggctgttttggcggatgagag	pWT057
WTP165	agctttccacggtggccgaccggtgcttg	
WTP166	gtcggccaccgtggaaagctttctgggttcaatcagg	
WTP167	aagcttcttaggtcgactcgtgcagccagt	
WTP172	ggaggcgtaataagaagcttggctgttttggcggatgagag	pWT059
WTP173	tcgtactcaaggtggccgaccggtgct	
WTP174	gtcggccaccttgagtacgagaccctgtccggcgagg	
WTP175	aagcttcttattacgcctcccccagcatccg	
WTP176	cccggcgtaataagaagcttggctgttttggcggatgagagaagattttcag	pWT060
WTP177	tctcggtcatggtggccgaccggtgct	
WTP178	gtcggccaccatgaccgagaccgtcaccgagac	
WTP179	aagcttcttattacgccgggacccaggc	
WTP180	gggcctatgataagaagcttggctgttttggcggatgagag	pWT061
WTP181	agaggctcatggtggccgaccggtgct	
WTP182	gtcggccaccatgagcctctcgaacctgggtcc	
WTP183	aagcttcttatcataggcccgcctccggc	
WTP184	ggcggcctagtaagaagcttggctgttttggcggatgagaga	pWT062

WTP185	aaatgcgcaaggtggccgaccggtgct	
WTP186	gtcggccaccttgcgcatttcgggaaccttgaacctct	
WTP187	aagcttcttactaggccgccttctggcgca	
WTP188	cgaagcggcccaccggtcggccaccatgg	pWT063
WTP189	cggtcatcacttaattcctcctgttagcccaaaaaacgggtatggaga	
WTP190	gaggaattaagtgatgaccgacaacaccgcgc	
WTP191	ccgaccggtgggccgcttcgctgacctgg	
WTP192	cgagtcgacccaccggtcggccaccatgg	pWT064
WTP193	agctttccacttaattcctcctgttagcccaaaaaacgggtatggaga	
WTP194	gaggaattaagtggaaagctttctgggttcaatcaggcagt	
WTP195	ccgaccggtgggtcgactcgtgcagccagttacg	
WTP200	cgccgcatcccaccggtcggccaccatgg	pWT066
WTP201	tggtggtcacttaattcctcctgttagcccaaaaaacgggtatggagaaacagtagag	
WTP202	gaggaattaagtgaccaccaacagcgcgacaag	
WTP203	ccgaccggtgggatgcggcgcgcgg	
WTP204	cggtcgtcgccaccggtcggccaccatgg	pWT067
WTP205	cggcgttcatttaattcctcctgttagcccaaaaaacgggtatggag	
WTP206	gaggaattaaatgaacgccgcgagcaagaaaatcc	
WTP207	ccgaccggtggcgacgaccgcgggtca	

WTP208	tgaggaagagcaccggtcggccaccatggtgagcaagggc	pWT068
WTP209	cggcgctcatttaattcctcctgttagcccaaaaaacgggtatggag	
WTP210	gaggaattaaatgagcgccgacgttcttgtgg	
WTP211	ccgaccggtgctcttcctcatcgccccgagcg	
WTP212	caacgccgcccaccggtcggccaccatgg	pWT069
WTP213	cgtccgacatttaattcctcctgttagcccaaaaaacgggtatggagaaacagtagagag	
WTP214	gaggaattaaatgtcggacgtcgaaaccacgc	
WTP215	ccgaccggtgggcggcgttggcggc	
WTP216	ggcgatccagcaccggtcggccaccatgg	pWT070
WTP217	gaagcgtcatttaattcctcctgttagcccaaaaaacgggtatggag	
WTP218	gaggaattaaatgacgcttcgcacccccg	
WTP219	ccgaccggtgctggatcgccttcgagacggcg	
WTP220	cccgctgagccaccggtcggccaccatgg	pWT071
WTP221	gttcggacaattaattcctcctgttagcccaaaaaacgggtatggag	
WTP222	gaggaattaattgtccgaacaactcgacgccgtggatgc	
WTP223	ccgaccggtggctcagcgggctgacatacgg	
WTP224	ggaagcgggccaccggtcggccaccatgg	pWT072
WTP225	gttttggtcatttaattcctcctgttagcccaaaaaacgggtatggag	
WTP226	ggaggaattaaatgaccaaaacggtccttgtcgtcga	

WTP227	ccgaccggtggcccgcttccttcatgtcgacttcg	
WTP228	ggaagagggccaccggtcggccaccatgg	pWT073
WTP229	ggtcggccatttaattcctcctgttagcccaaaaaacgggtatggagaaacagtagagag	
WTP230	gaggaattaaatggccgaccacgacgacc	
WTP231	ccgaccggtggccctcttcctcgtccggct	
WTP240	gaaggcggcccaccggtcggccaccatgg	pWT076
WTP241	aaatgcgcaattaattcctcctgttagcccaaaaaacgggtatggag	
WTP242	gaggaattaattgcgcatttcgggaaccttgaacc	
WTP243	ccgaccggtgggccgccttctggcgcac	
WTP001	aggcaagggctaaggatccgcggccgctga	pWT001
WTP002	cggatccttagcccttgccttccgaggcggc	
WTP106	aggcaagggctaaggatccgcggccgct	pWT037
WTP107	tgctcaccatgctagcgccctgaaaatacaggttttcactagt	
WTP108	gggcgctagcatggtgagcaagggcgaggag	
WTP109	cggatccttagcccttgccttccgaggcg	
WTP114	gctgtacaagtaaggatccgcggccgctgagcaa	pWT039
WTP115	tgctcaccatgctagcgccctgaaaatacaggttttcactagt	
WTP116	gggcgctagcatggtgagcaagggcgaggag	
WTP117	cggatccttacttgtacagctcgtccatgccgagag	

WTP268	aggcaagggctaaggatccgcggccgctgagcaataactagc	pWT086
WTP269	cggcgcccaaggtggccgaccggtgcttgtacagctcgtccatgccgag	
WTP270	gctgtacaagcaccggtcggccaccttgggcgccgtcgagactgcc	
WTP271	cggatccttagcccttgccttccgaggcg	
WTP449	ggatcagcgctaaggatccgcggccgctga	pWT141
WTP450	gcggatccttagcgctgatccagggcctggaa	
WTP451	acgttccagctaaggatccgcggccgctgag	pWT142
WTP452	gcggatccttagctggaacgttcgtggcgtt	
WTP455	gtcggccacccaggaactggtcgaccgcat	pWT144
WTP456	ccagttcctgggtggccgaccggtgcttgt	
WTP459	ggatcagcgccaggaactggtcgaccgcat	pWT146
WTP460	ccagttcctggcgctgatccagggcctggaac	
WTP534	gaacgttccagctaaggatccgcggccgctgagca	pWT170
WTP535	gcggatccttagctggaacgttcgtggcgtt	
WTP503	tcatcatcacatggtgagcaagggcgag	pWT154
WTP504	tcgggctttgctacttcttcttgaacaggcccgagaacatcg	
WTP505	gaagaagtagcaaagcccgaaaggaagctg	
WTP506	tgctcaccatgtgatgatgatgatgatggctgct	
WTP492	tcatcatcacatgggcagacacgggggg	pWT156

WTP493	tcgggctttgttacttgtacagctcgtccatgccgccgg	
WTP490	gtacaagtaacaaagcccgaaaggaagctgagttgg	
WTP494	gtctgcccatgtgatgatgatgatgatggctgctgccc	
WTP532	tcatcatcacaaggccgaggtcgcccatcg	pWT169
WTP533	gacctcggccttgtgatgatgatgatgatggc	
WTP552	ctcggggacgcggcgcctaacaaagcccgaaaggaagctg	pWT187
WTP553	tcctcgcccttgctcaccatgtgatgatgatgatgatggctgctgc	
WTP554	gccatcatcatcatcatcacatggtgagcaagggcgag	
WTP555	cagcttcctttcgggctttgttaggcgccgcgtccc	
WTP556	ccgtcggcgtgatggactaacaaagcccgaaaggaagct	pWT189
WTP557	acctgatgacgcggtttcatgtgatgatgatgatgatggctgctgcc	
WTP558	gccatcatcatcatcatcacatgaaaccgcgtcatcaggt	
WTP559	cagcttcctttcgggctttgttagtccatcacgccgacgg	
WTP560	ccgtcggcgtgatggactaacaaagcccgaaaggaagct	pWT150
WTP561	tcctcgcccttgctcaccatgtgatgatgatgatgatggctgctgc	
WTP562	gccatcatcatcatcatcacatggtgagcaag	
WTP563	acctgatgacgcggtttcatggtggccgaccggtg	
WTP564	acaagcaccggtcggccaccatgaaaccgcgtcatcaggt	
WTP565	cagcttcctttcgggctttgttagtccatcac	

WTP566	gctgtacaagtaacaaagcccgaaaggaagctgag	pWT190
WTP567	ccgaccggtggtccatcacgccgacgg	
WTP568	cgtgatggaccaccggtcggcc	
WTP569	ggctttgttacttgtacagctcgtccatgccg	
WTP574	agacgaccatatggtgagcaagggcgag	pWT205
WTP575	ccgaccggtgcttgtacagctcgtccatgcc	
WTP576	gctgtacaagcaccggtcggccac	
WTP577	tgctcaccatatggtcgtctccccaaaact	
WTP570	gaaggcaagggctaaaaaacgggcccccccctcga	pWT206
WTP571	ccgtttttttagcccttgccttccgaggcgg	
WTP578	gtcggccaccatgtccgatcag	pWT207
WTP579	gccaagcttcttaggcgccgcgtccc	
WTP580	cggcgcctaagaagcttggctgttttggcggatg	
WTP581	gatcggacatggtggccgaccggtg	
WTP582	gtcggccaccatggctatgaagctcgccgtca	pWT025
WTP583	caagcttcttatcagtagatcagttcgtcgtcgg	
WTP584	tgatctactgataagaagcttggctgttttggcg	
WTP585	tcatagccatggtggccgaccggtg	
WTP586	cgaggaaacgatggtgagcaagggcgag	pWT195

WTP587	ggcccgttttctacttcttcttgaacaggcccg	
WTP588	gaagaagtagaaaacgggcccccccctcg	
WTP589	tgctcaccatcgtttcctcgcatcgtgg	
WTP590	gtcggccaccatggctatgaagctcgccg	pWT200
WTP591	ccgttttctagtagatcagttcgtcgtcggc	
WTP592	actgatctactagaaaacgggcccccc	
WTP593	tcatagccatggtggccgaccggtg	
WTP598	gctgtacaagtaacaaagcccgaaaggaag	pWT209
WTP599	ggctttgttacttgtacagctcgtccatgc	
WTP693	tccaggccctggatcagcgctaagaagctt	pWT246
WTP694	gccaaaacagccaagcttcttagcgctgatcc	
WTP689	ggaaacgcatatggtgagcaagggcgagg	pWT243
WTP690	ccgctctagactactcttcgtcgctcacatcgg	
WTP691	cgaagagtagtctagagcggccattcactggcc	
WTP692	tgctcaccatatgcgtttcctcgcatcgtg	

Supplementary Table 6. Constructions of His-tagged proteins used in this study.

Protein	Synonyms	Mass (kDa)	Isoelectric point
PodJ_N	$PodJ_{1-601}$	68	4.93
SpmX(ΔTM)	$SpmX_{1-350}$	38.8	4.97
YFP		30.2	5.45
YFP-PodJ_N	YFP-$PodJ_{1-601}$	95.5	5.06
YFP-$PodJ_{CC1-3}$	YFP-$PodJ_{1-249}$	57.5	5.32
YFP-$PodJ_{CC4-6}$	YFP-$PodJ_{250-430}$	50.3	5.67
YFP-$PodJ_{IDR}$	YFP-$PodJ_{431-601}$	49.2	4.87
YFP-PodJ_N(ΔCC1-3)	YFP-$PodJ_{250-601}$	68.8	5.07
YFP-PodJ_N(ΔCC4-6)	YFP-$PodJ_{1-249, 431-601}$	76	4.92
YFP-PodJ_N(ΔIDR)	YFP-$PodJ_{1-430}$	77.1	5.44
mCherry		27.9	5.8
SpmX(ΔTM)-mCherry	$SpmX_{1-350}$-mCherry	66.1	5.22
PleC(ΔTM)-mCherry	$PleC_{307-842}$-mCherry	87.7	5.8
mCherry-CpaE		83.6	5.21

Supplementary references

1. Holehouse, A. S., Das, R. K., Ahad, J. N., Richardson, M. O. G., Pappu, R. V. CIDER: resources to analyze sequence-ensemble relationships of intrinsically disordered proteins. *Biophys. J.* **112**, 16-21 (2017).
2. Zhang, H., et al. Liquid-liquid phase separation in biology: mechanisms, physiological functions and human diseases. *Sci China Life Sci* **63**, 953-985 (2020).
3. Oshidari, R., et al. DNA repair by Rad52 liquid droplets. *Nat Commun* **11**, 695 (2020).
4. Lindner, A. B., Madden, R., Dernarez, A., Stewart, E. J., Taddei, F. Asymmetric segregation of protein aggregates is associated with cellular aging and rejuvenation. *Pro. Natl Acad. Sci. USA* **105**, 3076-3081 (2008).
5. Taylor, N. O., Wei, M.-T., Stone, H. A., Brangwynne, C. P. Quantifying dynamics in phase-separated condensates using fluorescence recovery after photobleaching. *Biophys. J.* **117**, 1285-1300 (2019).
6. Viollier, P. H., Sternheim, N., Shapiro, L. Identification of a localization factor for the polar positioning of bacterial structural and regulatory proteins. *Pro. Natl Acad. Sci. USA* **99**, 13831-13836 (2002).
7. Bowman, G. R., et al. A polymeric protein anchors the chromosomal origin/ParB complex at a bacterial cell pole. *Cell* **134**, 945-955 (2008).

8. Huitema, E., Pritchard, S., Matteson, D., Radhakrishnan, S. K., Viollier, P. H. Bacterial birth scar proteins mark future flagellum assembly site. *Cell* **124**, 1025-1037 (2006).

9. Radhakrishnan, S. K., Thanbichler, M., Viollier, P. H. The dynamic interplay between a cell fate determinant and a lysozyme homolog drives the asymmetric division cycle of *Caulobacter crescentus*. *Gene Dev* **22**, 212-225 (2008).